COMPRESSIVE DEFORMATION OF ZE41 MAGNESIUM ALLOY BETWEEN 23 AND 300 ℃

ZUZANKA TROJANOVÁ*, PAVEL LUKÁČ

Charles University, Faculty of Mathematics and Physics, Department of Metal Physics, Ke Karlovu 5, 121 16 Praha 2, Czech Republic

Received 19 October 2004, accepted 10 November 2004

The deformation behaviour of an Mg-Zn-RE (ZE41) magnesium alloy was investigated in uniaxial compression tests at temperatures between 23 and 300 ℃ and at an initial strain rate ranging from 2.7×10^{-5} to 1.3×10^{-2} s^{-1}. The yield stress of the alloy is very sensitive to the testing temperature. A local minimum in the temperature dependence of the yield stress was found at 100 ℃. The yield stress at 50 and 150 ℃ depends on the imposed strain rate, whereas it is practically independent of the strain rate at 100 ℃.

K e y w o r d s: magnesium alloy, mechanical properties, compression

1. Introduction

It is a great honour to write this paper to Professor Josef Čadek who has contributed very much to a better understanding of creep behaviour of many engineering alloys and composites. Aluminium-based and copper-based alloys and their composites also have been object of his study over last years (see e.g. [1–6]). His book Creep in Metallic Materials [7], is an excellent review on mechanisms of high temperature creep, creep damage, and creep fracture in metals and alloys. One can find there information suitable for interpretation of the mechanical properties obtained during deformation at a constant strain rate at elevated temperatures.

In contrast to aluminium and aluminium alloys, limited information is available on the deformation behaviour of magnesium alloys at elevated temperatures (above 20 ℃ = 293 K = 0.32 T_m, T_m is the absolute melting temperature). The differences in the deformation behaviour are influenced by the limited crystallographic slip systems in the hcp structure. In the last decade, a number of new magnesium alloy systems have been investigated and developed [8]. Magnesium-based

*corresponding author, e-mail: ztrojan@met.mff.cuni.cz

alloys exhibit high specific strength (the ratio of the yield stress to density) but the testing temperature influences significantly their deformation behaviour [9–13]. The strength of magnesium alloys at elevated temperatures increases if the alloys are reinforced with short fibres or small particles (see e.g. [14–16]). The use of equal channel angle pressing may improve the mechanical properties: an increase in the strength at 23 and 100 ℃ and an increase in the ductility at temperatures between 23 and 300 ℃ as was found for AZ91 magnesium alloy (e.g. [17]). Magnesium-based alloys also exhibit a high thermal conductivity and high coefficient of thermal expansion (CTE). The values of the CTE depend on the composition of Mg alloys and the composite components [18–20]. On the other hand, magnesium-based alloys possess a low corrosion resistance [21–23]. Aune and Westengen [24] have shown that Mg-Al-Si (AS41 and AS21) and Mg-Al-RE (AE41 and AE42) alloys exhibit major improvement in creep resistance due to a suppression of the formation of the $Mg_{17}Al_{12}$ phase. On the other hand, the yield strength of these alloys at higher temperatures is lower than that of Mg-9Al-1Zn alloy. Alloys containing zinc and rare-earth elements (RE), as for instance ZE41 magnesium alloy, exhibit moderate strength after ageing [8].

The aim of the present paper is to investigate the deformation behaviour in compression of a ZE41 alloy and to estimate the temperature and strain rate variation of the yield stress of the alloy.

2. Experimental procedure

The ZE41 alloy investigated in the present study has the following composition (in wt.%): Zn = 4, RE = Nd = 1, and Mg = balance. Test specimens were machined from the castings and they had a rectangular cross section of 6×6 mm^2 and a gauge length of 12 mm. Before testing, the specimens were subjected to T5 heat treatment (239 ℃/2 h, 177 ℃/16 h) according to [25].

Compression tests were performed in an Instron machine in the temperature range from 23 to 300 ℃ at various but constant crosshead speeds giving an initial strain rate between 2.7×10^{-5} and 1.3×10^{-2} s^{-1}.

3. Experimental results

Figure 1 shows the microstructure of the alloy studied in the condition after T5 heat treatment, revealing the α grains decorated by some phases. We suppose in agreement with [26] that these phases are a pseudoternary Mg-Zn-RE, exhibiting a wide range of composition.

Figure 2 shows the true stress-true strain curves obtained at various temperatures and at an initial strain rate of 1.3×10^{-4} s^{-1}. It can be seen that the flow stress is decreasing with increasing temperature at elevated temperature (excluding 100 ℃). The values of σ_{02} were determined as the flow stress at 0.2% offset strain

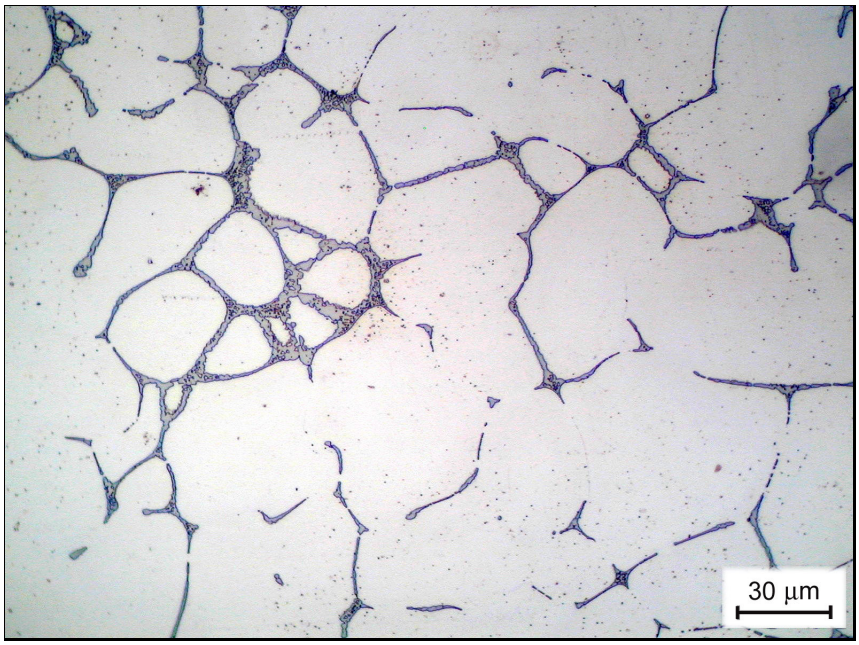

Fig. 1. Typical microstructure of the ZE41 alloy after heat treatment.

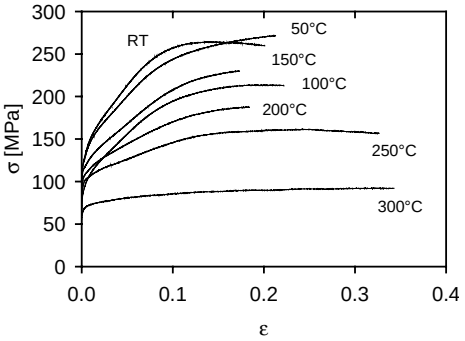

Fig. 2. True stress-true strain curves for ZE41 alloy at various temperatures and at a constant initial strain rate of 1.3×10^{-4} s^{-1}.

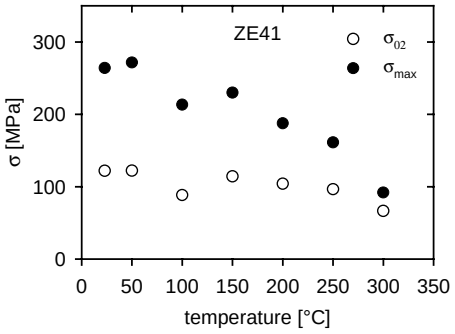

Fig. 3. Temperature dependence of the yield stress (empty circles) and the maximum stress (full circles).

and $\sigma_{\max}$ as the maximum flow stress. The variations of both the yield stress σ_{02} and the maximum flow stress $\sigma_{\max}$ as functions of temperature are shown in Fig. 3. It can be seen that the temperature variation of both σ_{02} and $\sigma_{\max}$ is complex.

The value of σ_{02} at room temperature is lower than that at 50 ℃ and the value of σ_{02} at 100 ℃ is significantly lower than that measured at 150 ℃. Similar conclusion is valid for $\sigma_{\max}$. By comparing the temperature variations of the values of σ_{02} and $\sigma_{\max}$ given in Fig. 3, it is evident that the temperature dependences of the yield stress and the maximum stress exhibit not only a local maximum at 50 ℃, which was recorded also in other magnesium alloys and in composites with the matrix of magnesium alloys (see e.g. [11, 12, 15, 16]). The dependences exhibit also a local minimum at 100 ℃. It should be noted that the measurements were repeated several times. This local minimum at 100 ℃ was also observed in Mg-0.7wt.%Nd when deformed at an initial strain rate of 3.3×10^{-4} s^{-1} [13]. The results indicate some dynamic strain ageing.

The strain rate dependences of the yield stress, $\sigma_{02,}$ at various temperatures are given in Fig. 4. It can be seen that the strain rate dependences have an anomalous course. The yield stress usually increases with increasing strain rate. In this case, the yield stress increases only at lower strain rates. At strain rates higher than 10^{-4} s^{-1}, the yield stress decreases with increasing strain rate at 50 and 150 ℃. At 100 ℃ the yield stress is independent of strain rate. Again, the results indicate some dynamic strain ageing. It is also obvious that the values of the yield stress at 100 ℃ are lower than those at 150 ℃ at all imposed strain rates (Fig. 4).

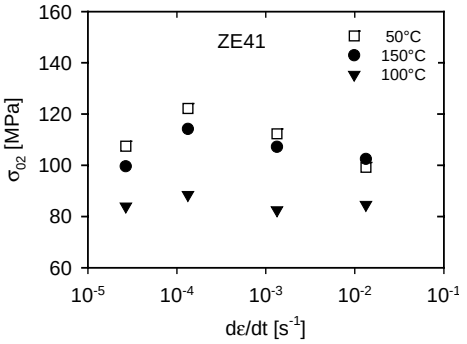

Fig. 4. Dependence of the yield stress on initial strain rate at various temperatures.

At elevated temperatures, the stress relaxation tests were performed at different strains during compression of the specimen. Fig. 5 shows the true stress-true strain curve obtained at 200 ℃ at an initial strain rate of 1.3×10^{-4} s^{-1}. During deformation, the testing machine was stopped at various strains (marked on the curve) and the specimen was allowed to relax. The stress relaxation was allowed to occur for 300 s. The flow stress after the stress relaxation, σ_1, was higher (or lower) than the flow stress at the beginning of the relaxation, σ_0. The values of $\Delta\sigma = \sigma_1 - \sigma_0$ are plotted against strain for two temperatures of 150 and 200 ℃ for an initial strain rate of 1.3×10^{-4} s^{-1} (Fig. 6). It can be seen that at the beginning of deformation the values of $\Delta\sigma$ are positive, then they decrease with strain and if the relaxation occurs at strains higher than a certain strain, the values of $\Delta\sigma$ are negative. It is evident that the values of $\Delta\sigma$ depend on strain and temperature for a constant time of relaxation.

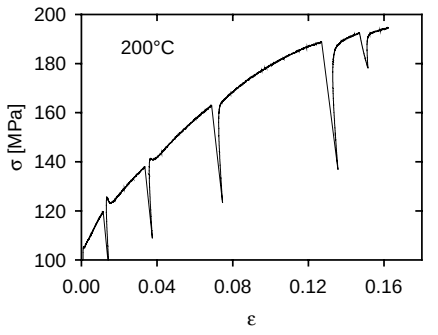

Fig. 5. A part of the true stress-true strain curves of ZE41 alloy deformed at 200 °C showing strains at which the stress relaxation tests were performed.

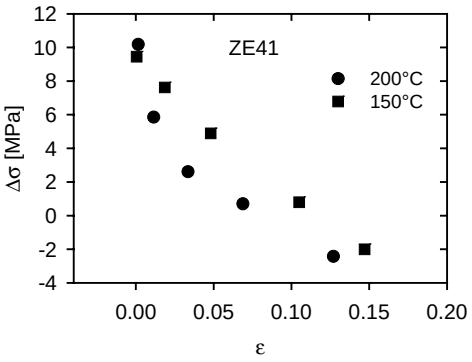

Fig. 6. Strain dependence of the difference in the flow stress at the beginning of deformation after stress relaxation and the flow stress at the beginning of the stress relaxation.

4. Discussion

The temperature dependences of the yield stress and the maximum stress of ZE41 magnesium alloy exhibit a hump between 100 and 150 °C. The strain rate dependence of the yield stress of the alloy has a negative slope in a certain strain rate range and at certain temperatures. The stress after stress relaxation at the beginning of deformation is higher than the stress at the beginning of the relaxation. The stress increase after relaxation depends on strain and temperature. From the results described above, it can be concluded that dynamic strain ageing causes the mentioned phenomena. It is known that the effects of dynamic strain ageing depend on temperature, strain rate and strain as well as on the concentration of solutes.

If specimens are deformed at certain elevated temperatures, the mobile dislocations drain solutes by pipe diffusion from the forest dislocation while they are waiting for thermal activation at the forest dislocations. During stress relaxation, solute atoms move to the moving dislocations. In this way, atmospheres of impurity atoms on dislocations are formed. The dislocations are pinned by the solutes. Therefore an increase in the stress is needed to move dislocations after reloading. It means the flow stress at the start of deformation after stress relaxation is higher. During strain, vacancies are formed. Their concentration depends on the strain and temperature. The generated vacancies enhance the solute diffusion.

The flow stress, necessary for the dislocation movement, may be expressed as a sum of two components

$$\sigma = \sigma_{\mathrm{d}} + \sigma_{\mathrm{f}}, \tag{1}$$

where σ_d is the dislocation component due to strong obstacles (e.g. forest dislocations, precipitates, grain boundaries) and σ_f is the friction stress due to the interaction between the solute atoms and moving dislocations.

According to Mulford and Kocks [27], it is the dislocation component of the flow stress rather than the friction stress that is affected by dynamic strain ageing. On the other hand, Balík and Lukáč [28] consider the influence of solute atoms on both components of the flow stress in dynamic strain ageing regime. The local solute concentration increment, Δc, can be expressed as

$$\Delta c = c - c_0 = \Delta c_M[1 - \exp(-t_w/t_0)^p], \tag{2}$$

where c is the local solute concentration in the dislocation core, c_0 is the nominal solute concentration in the matrix and Δc_M is the maximum concentration increment. The exponent $p = 2/(n + 2)$ and $1/(n + 2)$ for bulk and pipe diffusion, respectively. The value of n depends on the details of interaction between solute atom and dislocations. The exponent p is typically $2/3$ and $1/3$ for bulk and pipe diffusion, respectively. The relaxation time t_0 depends on the binding energy between a dislocation and a solute atom, on solute concentration, and on the diffusion coefficient of solute atoms. t_0 is inversely proportional to the diffusion coefficient in the case of bulk diffusion, whereas for pipe diffusion $1/t_0 \sim D\rho^{(n+2)/2}$ [29], where ρ is the density of forest dislocations.

The mean waiting time for successful activation, t_w, is connected with the strain rate by the Orowan equation

$$\dot{\varepsilon} = b\rho_m \Lambda / t_w = b\Omega / t_w, \tag{3}$$

where b is the magnitude of the Burgers vector, ρ_m is the mobile dislocation density, Λ is the mean free path of dislocations. If it is assumed that the forest dislocations are the rate controlling obstacles then $\Lambda = 1/\rho^{1/2}$. The elementary plastic strain per activation event $\Omega = b\rho_m\rho^{-1/2}$ is strain dependent; it may have a local maximum at a certain strain [30, 31].

The flow stress may be decomposed on a non-aged part σ_{na} and a dynamic strain ageing part σ_a, if it is considered that both the dislocation stress and the friction stress are influenced by solutes [28]. The strain rate dependence of the stress increment due to dynamic strain ageing is simply related to the kinetic law $\Delta c(t_w)$ – Eq. (2) – for the local concentration changes

$$\sigma_a = (f_1 + f_2)\Delta c(t_w). \tag{4}$$

The first term f_1 corresponds to the dislocation-dislocation interaction influenced by dynamic strain ageing and the second term f_2 results from the solute atoms-

-dislocation interaction influenced by dynamic strain ageing. Combining the relation (2) with the kinetic law (3), the negative strain rate dependence of the dynamic strain-ageing component is obvious. This causes the negative strain rate dependence of the yield stress, which is observed at certain temperatures and in a certain strain rate range (see Fig. 4).

The post stress relaxation effect – an increase or a decrease in the flow stress after the relaxation – may be described by a complex partial differential equation, as shown by Dlouhý et al. [32]. Solute atoms locking dislocations cause the stress increase after stress relaxation, which depends on strain and on temperature. An increase in the flow stress is needed to move the dislocations after stress relaxation. It is reasonable to assume that $\Delta\sigma$ is proportional to the number of impurities on dislocation lines. The density of dislocations increases with strain. But the concentration of solute atoms is constant. Thus, the stress increase, $\Delta\sigma$, after relaxation due to dynamic strain ageing should decrease with strain, which is observed. The value of Ω decreases with strain [30, 31] and hence, t_w also decreases. This leads to a decrease in $\Delta\sigma$ observed in the experiment.

During deformation, obstacles for moving dislocation are formed. At a sufficiently high strain, the moving dislocation can cross slip. Accordingly the strain hardening rate should decrease. Softening occurs. At higher temperatures and at higher strain, the activity of non-basal slip systems arises. Several dislocation reactions should be taken into account. Dislocations can be annihilated, which leads again to softening. Thus, the flow stress at the beginning of deformation after stress relaxation should be lower than the flow stress at the beginning of the relaxation [32], as observed at higher strains (Figs. 5 and 6).

5. Conclusions

It has been observed:

i) a hump in the temperature dependences of the yield stress and the maximum stress;

ii) a negative slope in the strain rate dependence of the yield stress in a certain strain rate range and temperatures;

iii) an increase in the flow stress after stress relaxation at certain strains.

The observed phenomena may be explained by dynamic strain ageing associated with solute atoms.

Acknowledgements

The authors are grateful for the financial support offered by the Grant Agency of the Academy of Sciences of the Czech Republic under Grant A2112303 and by the Grant Agency of the Czech Republic under Grant 106/03/0843.

REFERENCES

[1] KUCHAŘOVÁ, K.—ZHU, S. J.—ČADEK, J.: Kovove Mater., *40*, 2002, p. 69.
[2] ČADEK, J.—KUCHAŘOVÁ, K.: Kovove Mater., *40*, 2002, p. 133.
[3] KUCHAŘOVÁ, K.—ČADEK, J.: Kovove Mater., *40*, 2002, p. 231.
[4] ČADEK, J.—KUCHAŘOVÁ, K.: Kovove Mater., *41*, 2003, p. 127.
[5] ČADEK, J.—KUCHAŘOVÁ, K.: Kovove Mater., *42*, 2004, p. 9.
[6] ČADEK, J.—KUCHAŘOVÁ, K.—MILIČKA, K.: J. Alloys Comp., *378*, 2004, p. 123.
[7] ČADEK, J.: Creep in Metallic Materials. Amsterdam, Elsevier 1988.
[8] PEKGULERYUZ, M. O.—KAYA, A. A.: Adv. Eng. Mater., *5*, 2003, p. 866.
[9] LUKÁČ, P.—MÁTHIS, K.: Kovove Mater., *40*, 2002, p. 281.
[10] JÄGER, A.—LUKÁČ, P.—GÄRTNEROVÁ, V.: Kovove Mater., *42*, 2004, p. 165.
[11] TROJANOVÁ, Z.—LUKÁČ, P.—GÁBOR, P.—DROZD, Z.—MÁTHIS, K.: Kovove Mater., *39*, 2001, p. 368.
[12] DROZD, Z.—TROJANOVÁ, Z.—GÄRTNEROVÁ, V.: Magnesium Alloys and Their Applications. Ed.: Kainer, K. U. Weinheim, Wiley-VCH 2003, p. 122.
[13] TROJANOVÁ, Z.—GÄRTNEROVÁ, V.—PADALKA, O.: Kovove Mater., *42*, 2004, p. 206.
[14] TROJANOVÁ, Z.—KÚDELA, S.—LUKÁČ, P.—DROZD, Z.—PTÁČEK, L.—MÁTHIS, K.: Kovove Mater., *41*, 2003, p. 203.
[15] TROJANOVÁ, Z.—JÄGER, A.—DROZD, Z.: Kovove Mater., *42*, 2004, p. 214.
[16] TROJANOVÁ, Z.—GÄRTNEROVÁ, V.—LUKÁČ, P.—DROZD, Z.: J. Alloys Comp., *378*, 2004, p. 19.
[17] MÁTHIS, K.—MUSSI, A.—TROJANOVÁ, Z.—LUKÁČ, P.—RAUCH, E.: Kovove Mater., *41*, 2003, p. 293.
[18] LUKÁČ, P.—RUDAJEVOVÁ, A.: Kovove Mater., *41*, 2003, p. 281.
[19] RUDAJEVOVÁ, A.—GÄRTNEROVÁ, V.—JÄGER, A.—LUKÁČ, P.: Kovove Mater., *42*, 2004, p. 185.
[20] RUDAJEVOVÁ, A.—LUKÁČ, P.—KÚDELA, S.: J. Alloys Comp., *378*, 2004, p. 172.
[21] SONG, G.—ATRENS, A.: Adv. Eng. Mater., *5*, 2003, p. 837.
[22] HADZIMA, B.—PALČEK, P.—CHALUPOVÁ, M.—ČANÁDY, R.: Kovove Mater., *41*, 2003, p. 257.
[23] NEUBERT, V.—STULÍKOVÁ, I.—SMOLA, B.—BAKKAR, A.—MORDIKE, B. L.: Kovove Mater., *42*, 2004, p. 31.
[24] AUNE, T. K.—WESTENGEN, H.: SAE Technical Paper No. 950424, Detroit, Michigan, February 1995.
[25] ASM Specialty Handbook, Magnesium and Magnesium Alloys. Eds.: Avedesian, M. A., Baker, H. ASM International, Materials Park, OH 1999.
[26] WEI, L. Y.—DUNLOP, G. L.—WESTENGEN, H.: J. Mater. Sci., *32*, 1997, p. 3335.
[27] MULFORD, R. A.—KOCKS, U. F.: Acta Metall., *27*, 1979, p. 1125.
[28] BALÍK, J.—LUKÁČ, P.: Kovove Mater., *36*, 1998, p. 3.
[29] FRIEDEL, J.: Dislocations. Oxford, Pergamon Press 1964.
[30] KUBIN, L. P.—ESTRIN, Y.: Acta Metall. Mater., *38*, 1990, p. 697.
[31] BALÍK, J.—LUKÁČ, P.: Acta Metall. Mater., *41*, 1993, p. 1447.
[32] DLOUHÝ, A.—LUKÁČ, P.—TROJANOVÁ, Z.: Kovove Mater., *26*, 1984, p. 688.